Received 5 June 2023; accepted 3 July 2023. Date of publication 14 July 2023; date of current version 7 August 2023.

Digital Object Identifier 10.1109/OJAP.2023.3295423

A Technique to Realize Aperture Coupled Microstrip Patch as a Truly Low Cross-Polar Antenna by Mitigating the Major Issues Over Its Skewed Radiation Planes

SK RAFIDUL [1] (Graduate Student Member, IEEE), CHANDRAKANTA KUMAR [2] (Senior Member, IEEE), AND DEBATOSH GUHA [1,3] (Fellow, IEEE)

[1]Institute of Radio Physics and Electronics, University of Calcutta, Kolkata 700009, India

[2]Department of Space (Government of India), U R Rao Satellite Centre, Bengaluru 560017, India

[3]Department of Electronics and Communication Engineering, National Institute of Technology Jaipur, Jaipur 302017, India

CORRESPONDING AUTHOR: D. GUHA (e-mail: dguha@ieee.org)

This work was supported in part by the CSIR, Government of India and in part by the Scheme of Abdul Kalam Technology Innovation National Fellow of INAE/DST-SERB, Government of India.

ABSTRACT Aperture-fed microstrip patch is typically known for its low cross-polarized (XP) radiations, however it stands true only over its orthogonal plane. The same, over the diagonal planes are as high as that for any other common feeds. This specific issue has been addressed and successfully resolved by proposing a technique for the first time. This introduces a pair of additional printed loops adjacent to the radiating patch. Detailed investigations leading to the design insight have been presented. A C-band rectangular patch promises as much as 7 dB suppression in the diagonal plane XP level keeping the overall performance across the principal radiation planes unchanged. This is an important step in keeping the XP levels for an aperture-fed antenna truly low thus maintaining more than 22 dB of co- to cross-polar isolation over the entire azimuth.

INDEX TERMS Aperture fed patch, polarization purity, diagonal plane radiation, microstrip antenna.

I. INTRODUCTION

A POPULAR feed for a microstrip antenna consists of a coaxial probe, or a microstrip-line, or an aperture coupling [1]. Such feeds have relatively little control over the co-polarized (CoP) patterns but have a significant influence on the unwanted modes [2], [3], which cause cross-polarized (XP) radiations [4]. To address this issue in probe-fed geometries, several methods have already been explored, such as employing balanced feed [5], [6], [7], [8], [9], shaped and bulky ground planes [10], [11], [12], defected ground structure (DGS) [13], [14], [15], [16], [17], shorting pins [18], [19], [20], [21], [22], metasurfaces [23], etc. A few studies with microstrip feed can be found in [15], [17], and [24].

However, aperture-coupling has its own advantages. Its XP radiation is inherently low over both E- and H-planes [1], [4] and hence, it is considered an ideal candidate for dual-polarized applications [25], [26], [27]. However, this is a paradox since the XP level remains significantly high over the skewed planes that pass through around 45° azimuth. This is commonly known as a diagonal plane, or D-plane, and is frequently ignored. Such high XP levels sometimes impose limitations on antenna applications [28].

Indeed, these D-plane XP issues are not straightforward to deal with [28]. The sources behind such phenomenon were not known until the recent investigations in [16], [17], [29], [30]. According to [17], the D-plane XP fields do not originate from the so-called orthogonal mode; rather they are caused by antenna near fields. As a result, a balanced optimization of those source fields or their equivalent source currents (J_x, J_y, the primary resonance being x-polarized) becomes tricky.

This paper proposes a compensating current loop for an aperture-fed rectangular patch to obtain a balance between $\boldsymbol{J_x}$ and $\boldsymbol{J_y}$ and thus to minimize the target XP radiations over D-planes. A comprehensive design along with its physical insight has been presented. An experimental verification at C-band ensures about 6-7 dB reduction in D-plane XP level without compromising the primary radiation and other features of the antenna. This, to the best of our knowledge, is the first attempt without modifying or reshaping the ground plane to make an aperture-fed patch exhibit perfectly low XP over the entire radiation plane. Thus, it solves a longstanding issue and opens enough scopes for practical applications which demand higher cross-polar discrimination (XPD).

II. THE DIAGONAL PLANE ISSUES

This examination using [31] begins with three identical C-band patches fed by three different methods, as shown in Fig. 1. Their H- and D-plane radiation patterns are compared in Fig. 2. The patterns significantly vary only in terms of XP behavior. The H-plane feature is noticeable: the highest XP is produced by a probe-fed patch, which gets lowered by 5 dB in microstrip-fed geometry. It remarkably falls by another 10 dB when fed by aperture-coupling. This H-plane XP source is the weakly generated TM_{02} mode [28] due to a kind of perturbation caused by the feeding structure. Its impact is maximum when it is a vertical probe and moderate when it is a planar microstrip line. An aperture, in contrast, couples through an equivalent magnetic dipole and causes the least electrical perturbation. Its H-plane XP thus becomes inherently low. But the scenario is completely different in D-plane. Apart from an asymmetry imposed by the vertical probe, the peak XP levels caused by all three configurations seem to be mutually comparable. Their peaks around 45° are predominantly high, say by about −6 to −8 dBi. Such D-plane behavior prevents its application as a true low-XP device, even if it offers so impressive features over the H-plane.

III. THE DESIGN APPROACH AND INSIGHT

The definition of XP fields was provided in [32]. Their predominant components occurring across the orthogonal and diagonal radiation planes can be expressed as [16]:

$$\text{For } \varphi = 90^\circ,\ \boldsymbol{E_{xp}} = E(\theta, 90^\circ)\{(\cos\theta)\widehat{\boldsymbol{\iota}_y}\} \quad (1)$$

$$\text{For } \varphi = 45^\circ,\ \boldsymbol{E_{xp}} = 0.5E(\theta, 45^\circ) \times \left[(1+\cos\theta)\widehat{\boldsymbol{\iota}_y} - (1-\cos\theta)\widehat{\boldsymbol{\iota}_x}\right] \quad (2)$$

where, $\widehat{\boldsymbol{\iota}_x}$, $\widehat{\boldsymbol{\iota}_y}$ are the source current polarizations vectors and θ is the elevation angle. These $\widehat{\iota}$ vectors indeed align with the associated surface currents $\boldsymbol{J} = \nabla_{\boldsymbol{n}} \times \boldsymbol{H}$ with $|\boldsymbol{H}| = |\boldsymbol{E}|/\eta$. Thus, $\boldsymbol{J_y}$ appears to be the primary contributor to the XP fields in both planes and $\boldsymbol{J_x}$ plays a role over the D- plane only. The best way of controlling it is to maximize $\boldsymbol{J_x}/\boldsymbol{J_y}$ ratio since $\boldsymbol{J_x}$ is indispensable in terms of the main radiation. The proposed method introduces a pair of resonant loops adjacent to the patch as shown in Fig. 3. The idea is to get it electromagnetically coupled with the patch, resonate at the same frequency, and enhance the effective conduction current along the x-axis as well as reduce along the y-axis. Thus, the loop perimeter $2(a + b)$ becomes strategic to match with λ_{av} ($\approx (\lambda_0 + \lambda_g)/2$). It may be noted that the overall deployment area of the proposed looped coupled patch is conveniently accommodated within $\lambda_0 \times \lambda_0$ GP. This indeed is found to be the optimum GP dimension required for maximum gain

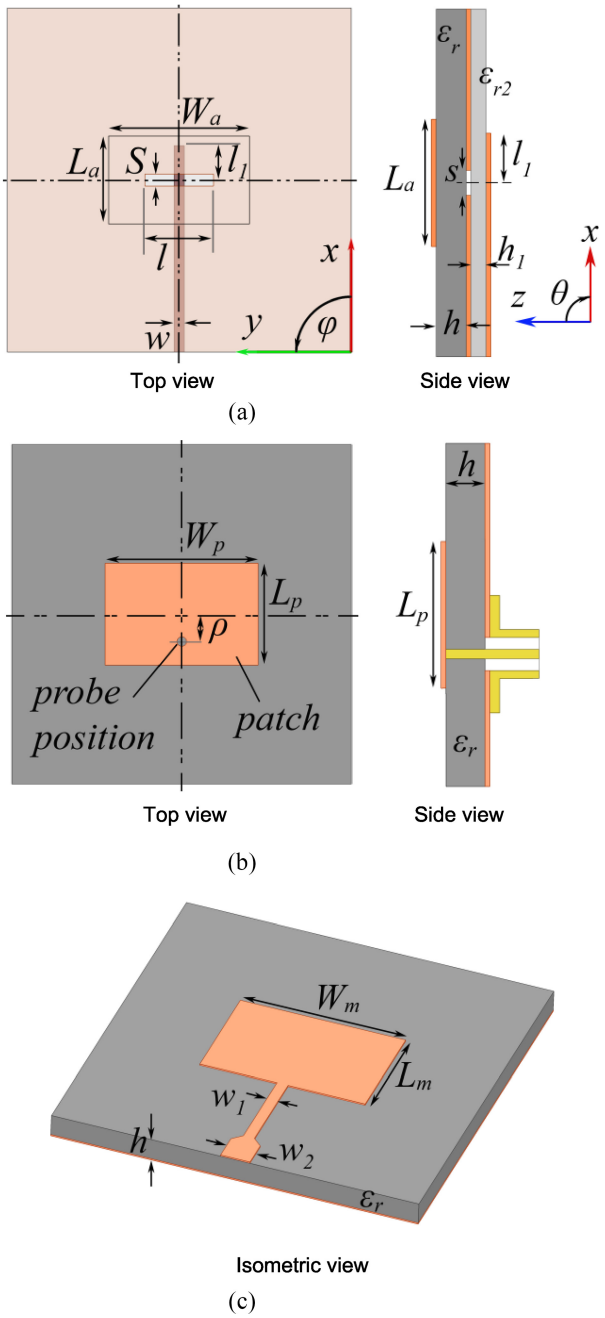

FIGURE 1. Rectangular microstrip patches with different feeds: (a) aperture coupled fed, (b) probe fed, and (c) microstrip fed. L_a = 12.8, W_a = 20.48, w = 1.5, l = 10, s = 1.75, l_1 = 11, L_p = 14.34, W_p = 22.94, ρ = 3.85, L_m = 14.05, W_m = 22.48, w_1 = 1.4, w_2 = 4.7; substrate: ε_r = 2.33, h = 1.575, ε_{r1} = 2.2, h_1 = 0.508; ground plane 50 × 50, all dimensions in mm.

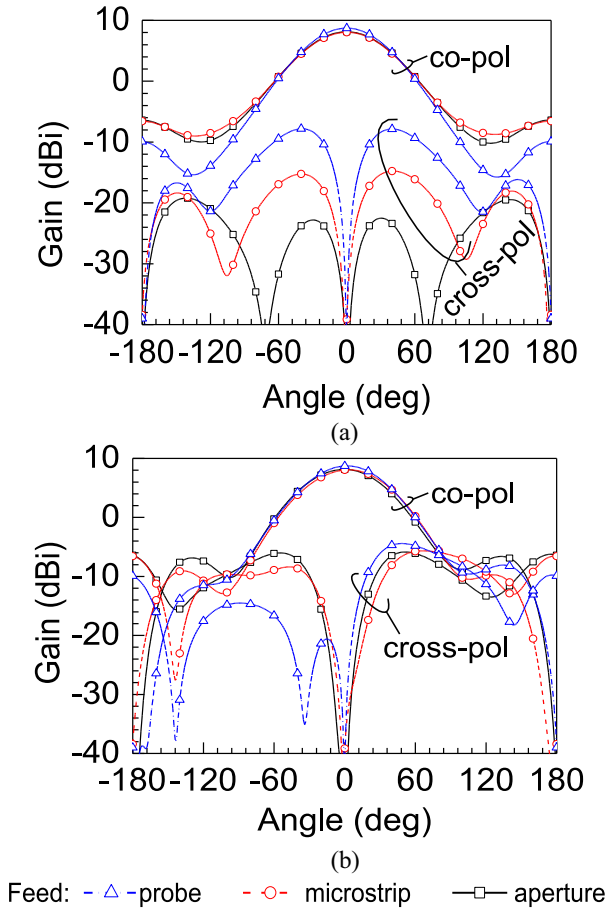

FIGURE 2. Radiation characteristics of the rectangular patch for three different feeding techniques: (a) H-plane, (b) D-plane. Parameters as in Fig. 1.

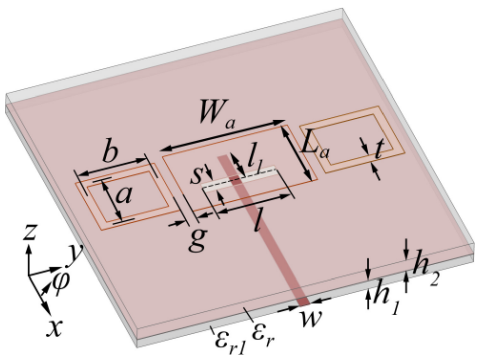

FIGURE 3. Configuration of an aperture-coupled patch integrated with loops.

with minimum XP. A detailed study will be provided in Section IV.

The magnitude of $\boldsymbol{J_x/J_y}$ over the entire GP of a conventional patch is shown in Fig. 4(a). It is equally high across both co- and cross-polar axes and endorses the reality of occurring low H-plane XP values, as obtained in the aperture-coupled version of Fig. 2(a). The physical meaning of the same can be visualized from the simulated current vectors of Figs. 4(b) and (c). However, $\boldsymbol{J_x/J_y}$ in Fig. 4 (a) is found to be noticeably low over the diagonal axes. Our present approach

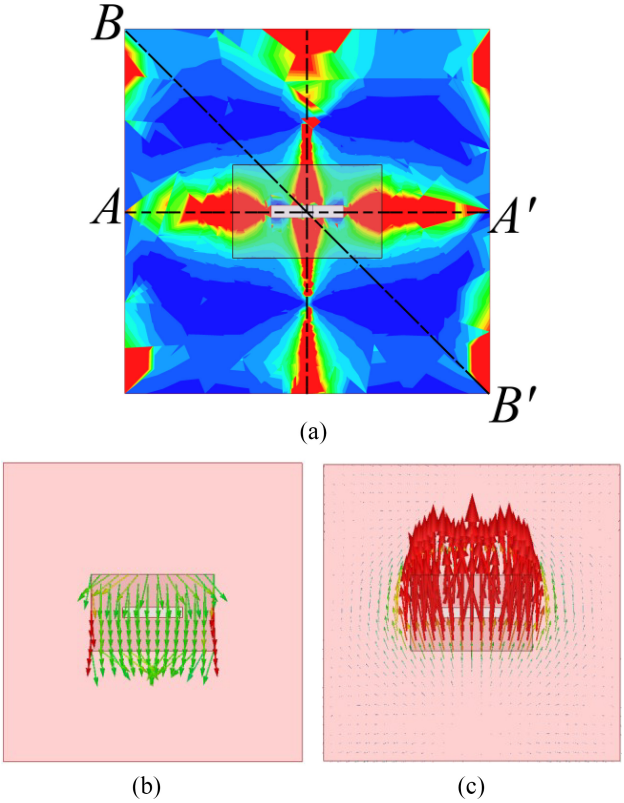

FIGURE 4. Simulated portrays of conduction currents for a conventional geometry: (a) magnitude of J_x/J_y on the ground, (b) current vector on patch surface, (c) resulting current vector on GP. Parameters as in Fig. 1.

is to enhance $\boldsymbol{J_x/J_y}$ ratio, especially around the diagonal axes (BB′). This is possible either by decreasing J_y or by increasing J_x. Newly introduced EM coupled loops indeed make it happen. Fig. 5 helps in understanding the situation. The coupling phenomenon between the patch edges and the loops redistributes the conduction currents. Their simulated and equivalent schematic portrays are shown through Figs. 5(a) and (b) respectively. It is clearly evidenced from Fig. 5(a) that the resonating nature of the loops creates a situation where J_y components turn mutually opposite in phase and cancel out. The J_x components in contrast get widely redistributed and add up. This eventually enhances $\boldsymbol{H_y}$ across AA′ (Fig. 5(c)). Its physical manifestation is examined in Fig. 6. The GP current remains predominantly x-polarized and gets widely distributed compared to that occurring underneath a standalone patch (Fig. 4(c)). Finally, Fig. 6(b) depicts simulated values of $\boldsymbol{J_x/J_y}$ which compared to Fig. 4(a) appears distinctively improved covering a wider zone of the radiating aperture. Improved $\boldsymbol{J_x/J_y}$ especially around BB′ should have a considerable impact in reducing XP fields across the skewed radiation planes.

IV. RESULTS AND VERIFICATIONS

The proximity of the loops has to be maintained as $g \approx 0.01\lambda_{av}$. The overall resonance, as studied in Fig. 7(a),

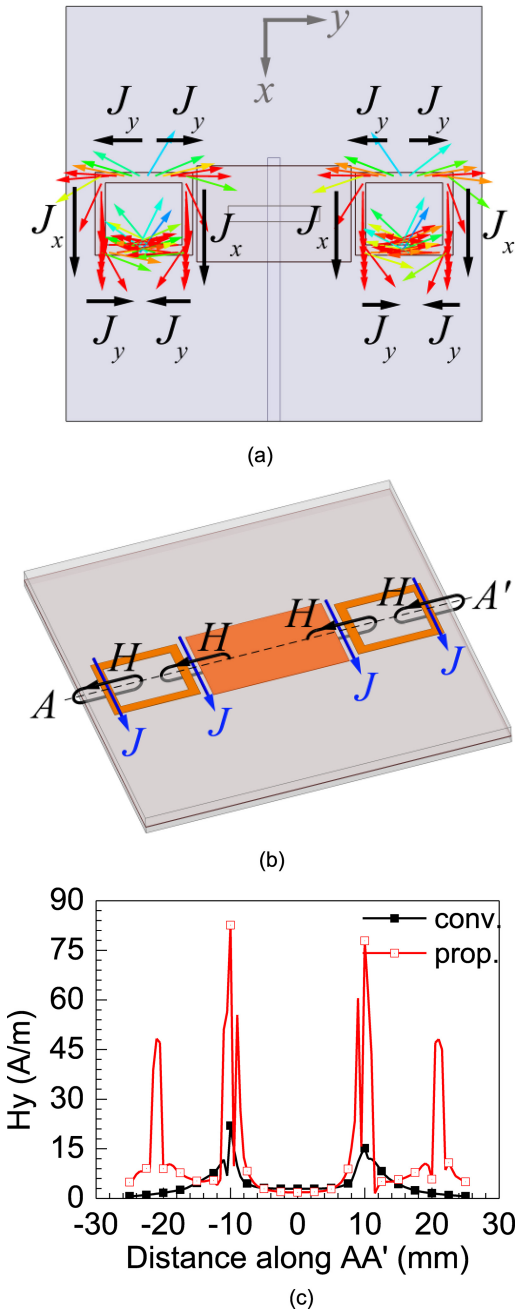

FIGURE 5. Impact of coupling between patch and loops: (a) simulated current, (b) equivalent current and H-fields, and (c) |Hy| distribution along AA′. Parameters: $L_a = 11.6$, $W_a = 18.56$, $w = 1.5$, l = 11, $s = 1.9$, $l_1 = 6.75$, $g = 0.6$, a = 8.75, $b = 10.5$, t = 1.25. Other parameters as in Fig. 4.

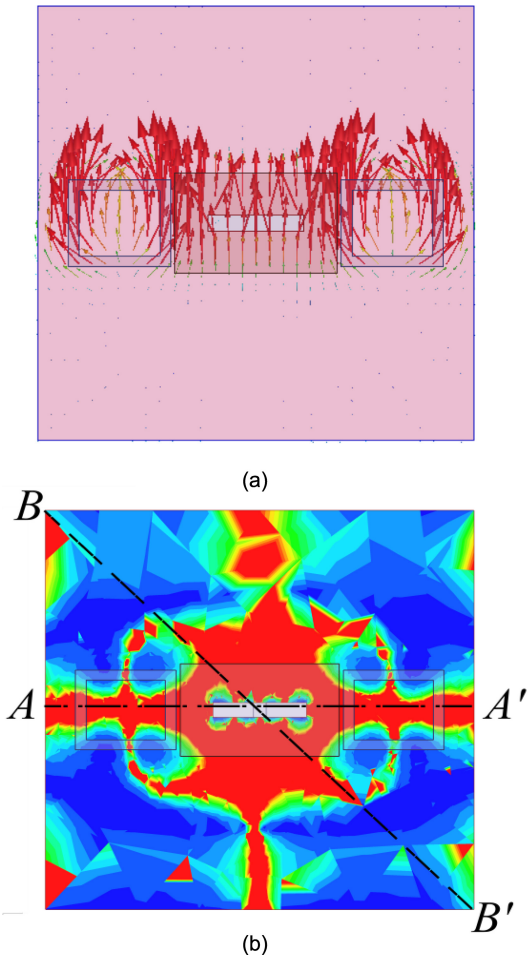

FIGURE 6. Surface current scenario for the proposed loop coupled patch: (a) simulated current vectors, (b) magnitude of Jx/Jy distributed over the ground plane. Parameters as in Fig. 5.

significantly depends on the value of a, the optimum perimeter ($2a + 2b$) being unaltered. Typically, $a < L_a$ and for this specific design $a \approx 0.75L_a$ shows the best possible matching.

The patch gets capacitively coupled with the loops causing a left shift of the resonance and hence an adjustment is required by changing the patch dimension. Figs. 7(b) and (c) examine the radiation properties. The CoP patterns remain close to those caused by an isolated patch except a small reduction in beam-width over H-plane. The expansion of effective aperture caused by the loops is the reason behind this, resulting in an increase in gain by 1.2 dB. More significantly, the targeted achievement over the D-planes is enormous: the XP level reduces from −6 dBi to −13 dBi as evident from Fig. 7(b). E-plane XP values for both geometries are inherently low (below −35 dBi) and hence are not discussed here. It is also important to note that the role of a in controlling radiation patterns is not as sensitive as observed in guiding S_{11} in Fig. 7(a). Therefore, $a = 8.75$ mm $\approx 0.75L_a$ appears to be the best acceptable value. With this a, H-plane XP level is found to rise marginally from −25 dBi to −24 dBi. However, it still remains significantly lower when compared to the values observed in the D-plane. One can visualize the actual impact from the 3D XP patterns as documented in Fig. 8. Both patterns are displayed with identical physical and color scales. The conventional patch (Fig. 8(a)) reveals a very low XP level over the principal planes (xz and yz) and significantly high values over the D-planes ($\varphi = 45°$). The same gets a drastic reduction (Fig. 8(b)) when the proposed design is implemented. Our study ensures a maximum of 6-7 dB improvement in the 3D XP scenario.

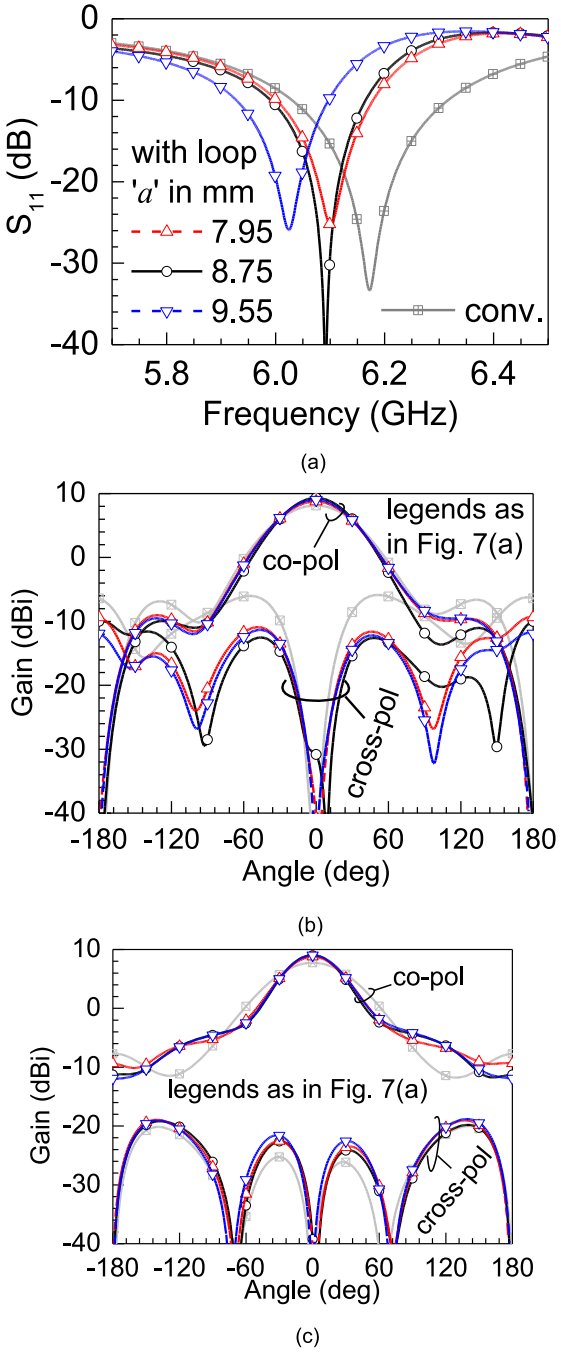

FIGURE 7. Simulated characteristics of the antennas with and without loops: (a) S_{11} versus frequency and radiation patterns in (b) D-plane, (c) H-plane. Parameters as in Fig. 5.

This eventually reveals CoP to XP isolation over 22 dB across all radiation planes.

A relative performance of the proposed configuration as a function of GP size is examined in Fig. 9. Indeed, a conventional patch with a GP below 0.9λ does not appear useful because of lower gains. Hence, the range of the present study is from 0.9λ to 1.3λ, which comfortably accommodates the proposed loop coupled patch. The said GP size reveals consistent improvements both in D-plane XP and peak gain.

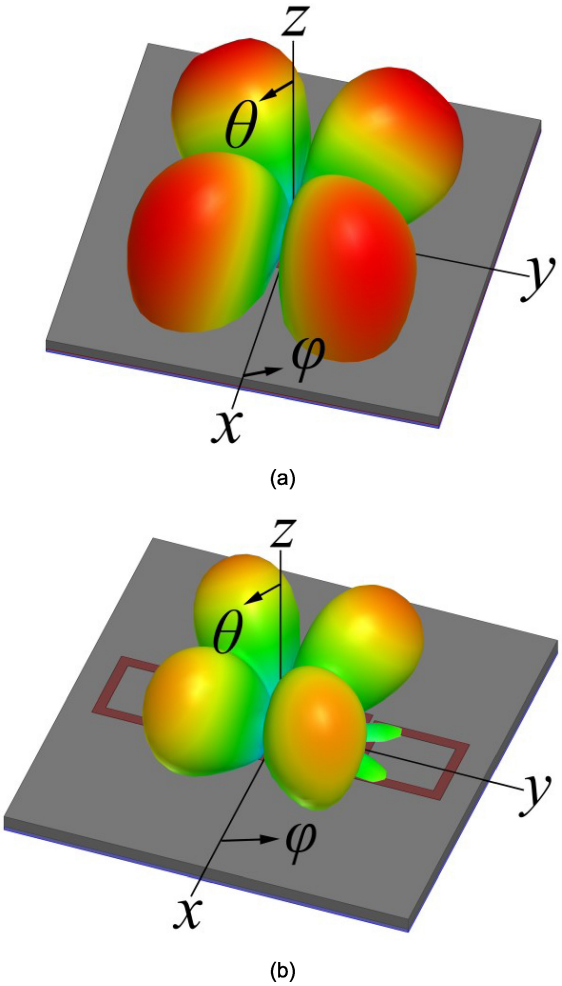

FIGURE 8. 3D scenario of XP levels at resonance: (a) conventional, and (b) proposed, both in identical physical/color scales. Red: maximum, Green: minimum. Parameters as in Fig. 5.

From the nature of variation (Fig. 9), one may surmise the optimum GP size of the order of λ.

The concept of the loop has been reconfirmed by changing its shape from rectangle to circle as shown in Fig. 10(a). The impedance and radiation performances appear mutually comparable and a representative comparison for D-plane radiation patterns is shown in Fig. 10(b). The rectangular loop appears a bit compact relative to the circle and is hence a better choice for practical applications. It may be noted that in realizing an array each of the loops should serve a pair of adjacent elements and thus no extra space is required to accommodate the loop in between two radiating elements.

V. PROTOTYPES AND MEASUREMENTS

A set of prototypes with and without loops are realized and the photograph for the proposed geometry is shown in Fig. 11(a). Agilent's E8363B precision network analyzer and an anechoic chamber provided with an MI-750 microwave receiver have been used for the measurements. A pyramidal horn with more than 40 dB XP isolation was used as the transmitting radiator.

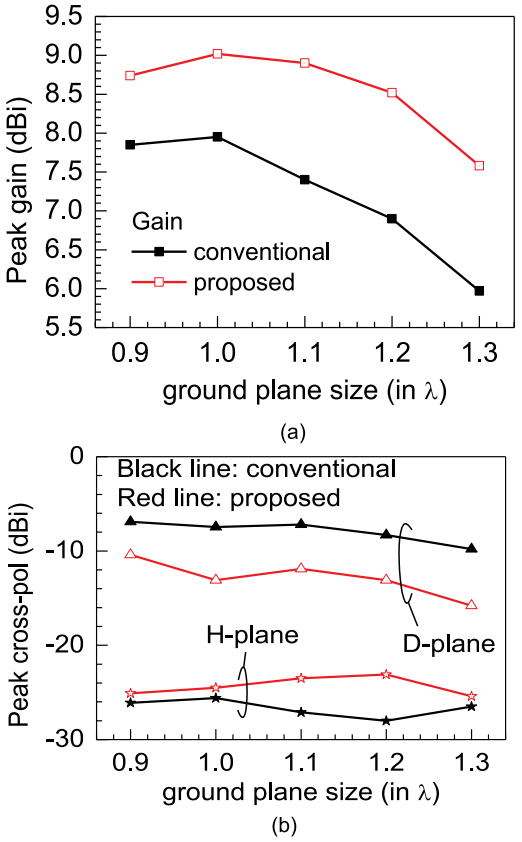

FIGURE 9. (a) Peak gain and (b) peak XP variation in proposed and conventional antenna as a function of GP size. Parameters as in Fig. 5.

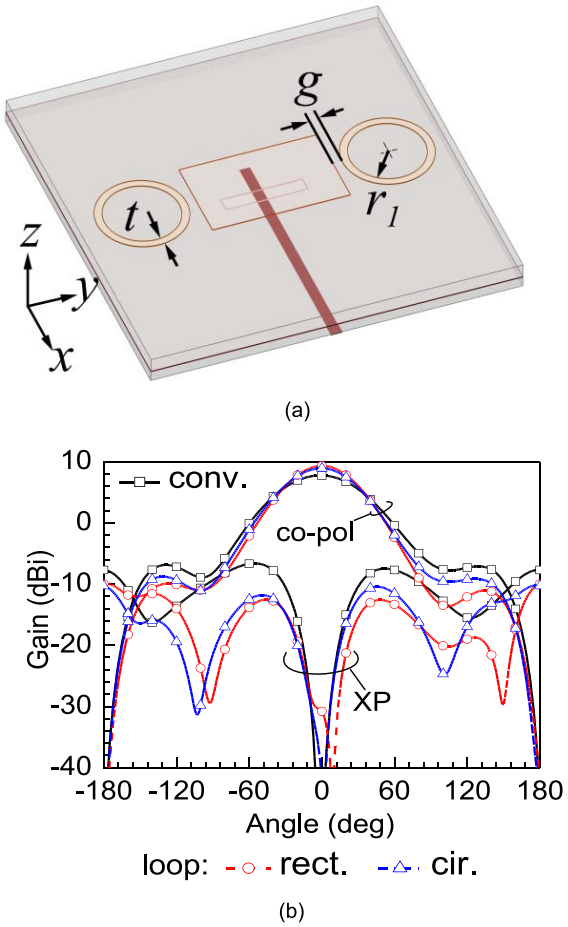

FIGURE 10. Circular loop tested with the same patch: (a) the layout, (b) comparison of D-plane radiation patterns obtained using [31]. Parameters: $r_1 = 5.1$ mm, $t = 1.25$ mm, $g = 0.32$ mm, $l_1 = 6.5$ mm, and the rest as in Fig. 5.

Fig. 11(b) examines their measured S_{11} in comparison with the simulated predictions. Satisfactory impedance matching is evident. The antenna with loops reveals a relatively narrower matching bandwidth. Their radiation patterns across the planes of our interest are shown in Fig. 12 ensuring very close agreement between the measured and simulated data. The measured peak gain of the proposed geometry with loops is found to be 9.1 dBi, which appears improved by about 1 dB compared to that without loop. This gain increment is associated with a minor decrement in beam width. As predicted for H-plane (Fig. 12(a)), the measured XP levels also show no considerable difference between the configurations with and without loops. Fig. 12(b) indeed experimentally establishes the design target that, D-plane XP values get reduced by about 7 dB over a wide angular range around the boresight. This indeed results in more than 14 dB XPD which is significant to a scanning beam array generating its beams covering the diagonal planes. The consistency of this feature over the entire operating band has been ensured by repeating the measurements as furnished through Fig. 13. Near the lower edge of the band ($f = 6.02$ GHz), the order of XP reduction is about 4 dB which increases up to 7 dB at the upper edge ($f = 6.21$ GHz). Table 1 provides a comprehensive overview of the peak gain and XP levels at resonance for the antenna, allowing for a clearer understanding of the performance differences between the configurations with and without loops. One can estimate the improvement in the XP discrimination over the D-plane as 7 dB.

TABLE 1. Comparison of peak gain and XP level of the antenna with and without loops.

Antenna type	Peak gain (dBi)	Peak XP level (dBi)		
		E-plane	H-plane	D-plane
Without loop	7.9	-35	-25	-6
With loop	9.0	-35	-25	-13

TABLE 2. Measured radiation efficiency of the prototypes.

Antenna type	R_t(Without cap) (Ω)	R_t(With cap) (Ω)	η (%)
Without loop	42.3	5.2	87.7
With loop	48.5	6	87.6

VI. RADIATION EFFICIENCY

The loop hardly causes any change in the antenna efficiency, confirmed by the measured values obtained using Wheeler cap method [33]. The technique uses measured input resistance of the antenna at resonance with and without Wheeler

TABLE 3. Proposed investigation compared with earlier reported works.

Investigation		CoP-to-XP Isolation (dB)		Peak Gain (dBi)	Volume ($l \times w \times h$) in λ^3	Comments
		H-plane	D-plane			
Balance feeding	[6]	23	*	7.2	$\pi \times (0.46)^2 \times 0.95$	Complicated fabrication.
	[7]	22	*	4.2	$1.2 \times 1.2 \times 0.01$	
GP shaping	[10]	20	*	8	0.45×0.83×0.16	Bulky Structure, not effective over D-plane
	[11]	19	*	9.5	0.8×0.85×0.4	
DGS Based Design	[13]	16.5	*	6.5	1.66×1.66×0.083	Considerable back radiation with some degree of lower gain.
	[16]	28	25	8.0	1 ×1 × 0.03	
	[17]	30	22	8.1	1 ×1 × 0.03	
Shorting Pin/wall	[19]	25	*	7.7	$1.8 \times 1.8 \times 0.05$	Not effective over the D-plane
	[20]	32	*	7.5	$2 \times 2 \times 0.05$	
Present		**35**	**22**	**9.1**	**1 × 1 × 0.04**	Low XP across all radiation planes, good gain, no back radiation, easy to implement.

* D-plane not addressed

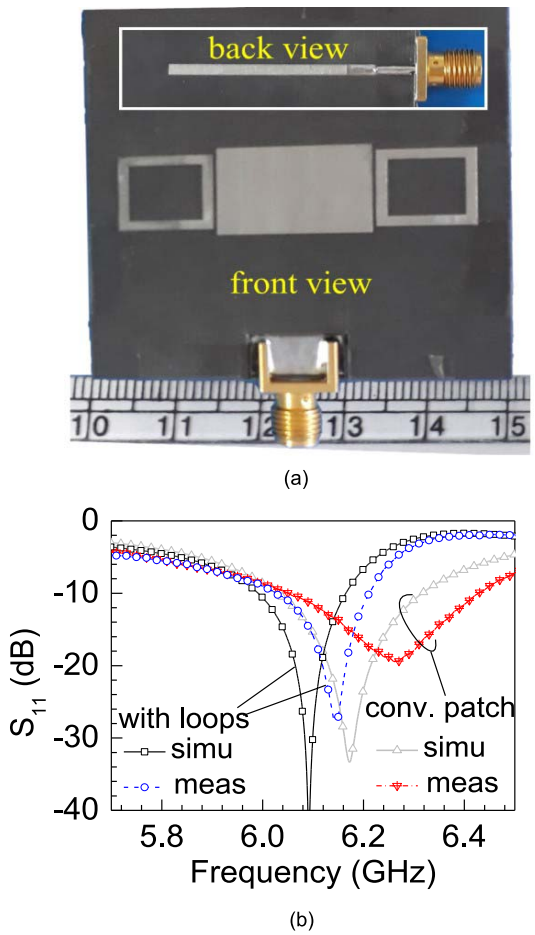

FIGURE 11. (a) Prototype of the proposed geometry, the feed line in the inset; (b) measured and simulated S_{11} of the prototypes. Parameters as in Fig. 5.

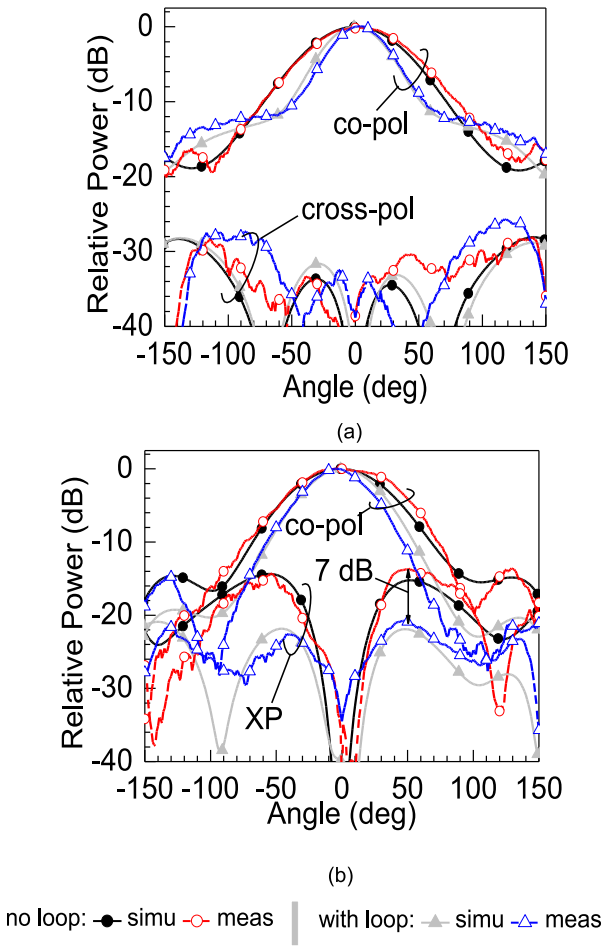

FIGURE 12. Measured and simulated radiation patterns of the prototypes as in Fig. 10 at the respective band-center: (a) H-plane, and (b) D-plane. Parameters as in Fig. 5.

cap. The cap is actually a metallic shield that covers the antenna under test and prevents radiation from it [34]. This will be evident from our experimental setup as depicted through Fig. 14. The radiation efficiency is calculated as [33]

$$\eta = \left(\frac{Radiated\ Power}{Total\ Input\ Power}\right) \times 100\% \quad (3)$$

$$= \frac{R_r}{R_t} = \frac{R_t - R_l}{R_t} \times 100\% \quad (4)$$

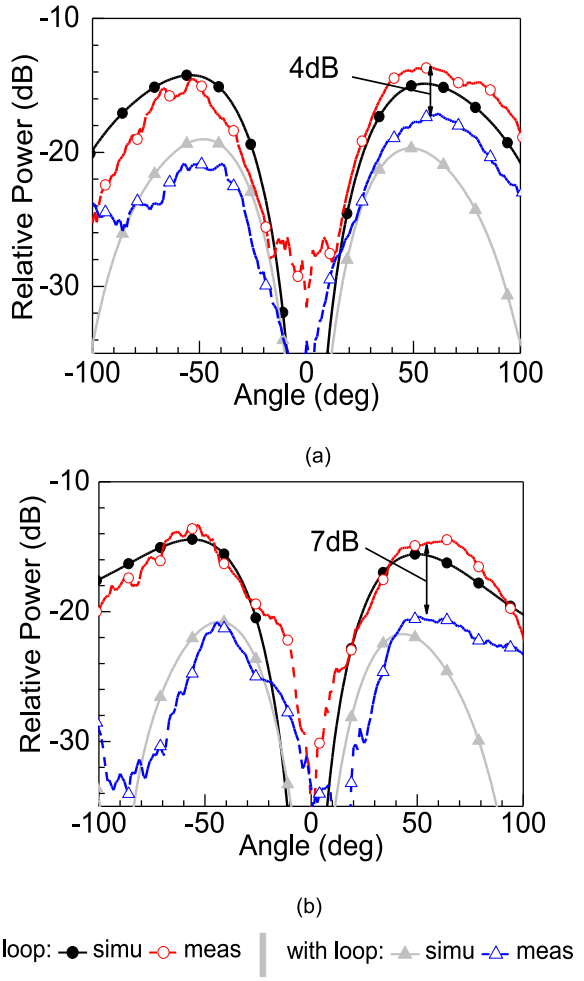

FIGURE 13. Measured D-plane XP at (a) lower edge and (b) upper edge of the operating band. Parameters as in Fig. 5.

where, the total resistance (R_t) = radiation resistance (R_r) + loss resistance (R_l). Their measured values and obtained efficiencies with and without loops are documented in Table 2. The measured efficiencies hardly show any noticeable change caused by the introduction of the loops.

VII. POSSIBILITY IN ARRAY CONFIGURATION

This work examines the suitability of the proposed geometry in an array configuration. An H-plane array in Fig. 15(a) indicates that each loop serves two adjacent elements and therefore, the inter-element spacing becomes 0.63λ (with W/L = 1.6) which is reasonably acceptable for a practical design. It is possible to meet 0.5λ spacing by adjusting the W/L ratio. Its impedance property is compared with the standalone antenna in Fig. 15(b) indicating a marginal enhancement by 40 MHz. The radiation characteristics of the array examined over both D- and H-planes (Fig. 16) promise considerable improvement in terms of polarization purity, as in the case of a single-element study.

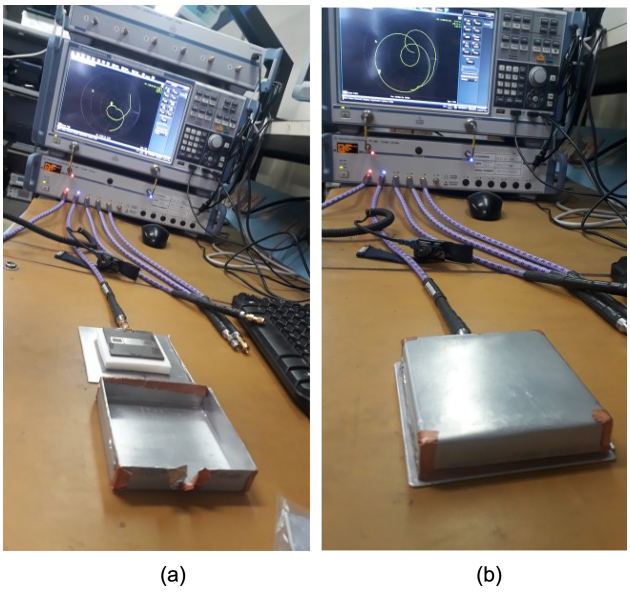

FIGURE 14. Experimental set-up of the Wheeler cap measurement technique. (a) antenna without Wheeler cap, (b) antenna with Wheeler cap.

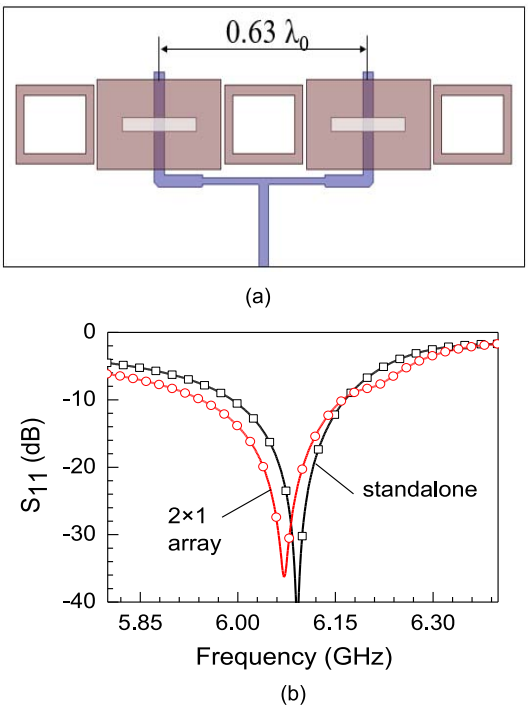

FIGURE 15. (a) Application of the loops in a 2 × 1 array and (b) its S_{11} response in comparison with a standalone patch. Element parameters as in Fig. 5.

VIII. CONCLUSION

This investigation shows how an aperture-fed microstrip patch could be made to qualify as a truly low cross-pol antenna. The new technique without adding extra cost or complexity has been successfully demonstrated for the first time. The typical overall dimension of a standalone antenna appears adequate to accommodate the loops. The antenna structure, therefore, does not demand any extra space or size.

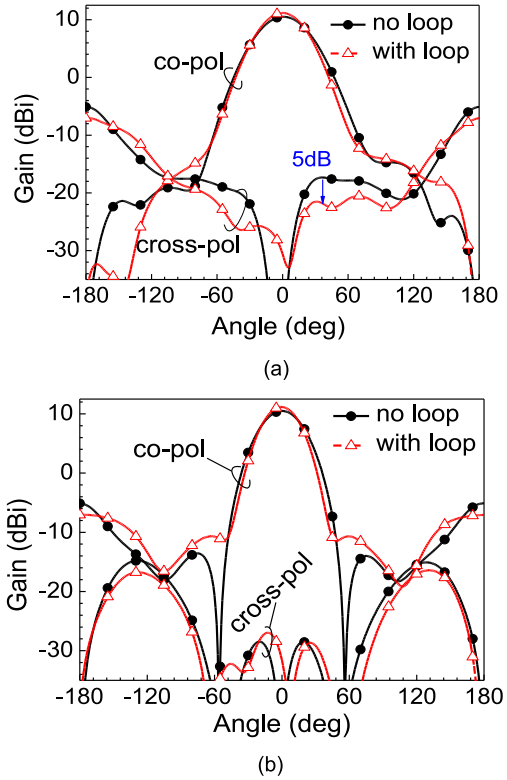

FIGURE 16. Simulated radiation patterns of the arrays with and without loops as in Fig. 15 at the resonance frequency: (a) D-plane, (b) H-plane. Element parameters as in Fig. 5.

A comprehensive comparison is provided in Table 3 indicating adequately improved and useful features. It should find potential applications in base station repeater and telemetry downlink systems.

REFERENCES

[1] R. Garg, P. Bhartia, I. J. Bahl, and A. Ittipiboon, *Microstrip Antenna Design Handbook*. Norwood, MA, USA: Artech House, 2001.

[2] J. Huang, "The finite ground plane effect on the microstrip antenna radiation patterns," *IEEE Trans. Antennas Propag.*, vol. AP-31, no. 4, pp. 649–653, Jul. 1983.

[3] R. C. Hansen, "Cross polarization microstrip patch antennas," *IEEE Trans. Antennas Propag.*, vol. AP-35, no. 6, pp. 731–732, Jun. 1987.

[4] D. Guha and C. Kumar, "Microstrip patch versus dielectric resonator antenna bearing all commonly used feeds: An experimental study to choose the right element," *IEEE Antennas and Propag. Mag.*, vol. 58, no. 1 pp. 45–55, Feb. 2016.

[5] A. Petosa, A. Ittipiboon, and N. Gagnon, "Suppression of unwanted probe radiation in wideband probe-fed microstrip patches," *Electron. Lett.*, vol. 35, no. 5, pp. 355–357, Mar. 1999.

[6] P. Li, H. W. Lai, K. M. Luk, and K. L. Lau, "A wideband patch antenna with cross-polarization suppression," *IEEE Antennas Wireless Propag. Lett.*, vol. 3, pp. 211–214, 2004.

[7] Y. P. Zhang, "Design and experiment on differentially-driven microstrip antennas," *IEEE Trans. Antennas Propag.*, vol. 55, no. 10, pp. 2701–2708, Oct. 2007.

[8] H. Jin, K.-S. Chin, W. Che, C.-C. Chang, H.-J. Li, and Q. Xue, "Differential-fed patch antenna arrays with low cross polarization and wide bandwidths," *IEEE Antennas Wireless Propag. Lett.*, vol. 13, pp. 1069–1072, 2014.

[9] H. Saeidi-Manesh and G. Zhang, "High-isolation, low cross-polarization, dual-polarization, hybrid feed microstrip patch array antenna for MPAR application," *IEEE Trans. Antennas Propag.*, vol. 66, no. 5, pp. 2326–2332, May 2018.

[10] W.-H. Hsu and K.-L. Wong, "Broadband probe-fed patch antenna with a U-shaped ground plane for cross-polarization reduction," *IEEE Trans. Antennas Propag.*, vol. 50, no. 3, pp. 352–355, Mar. 2002.

[11] K.-L. Wong, C.-L. Tang, and J.-Y. Chiou, "Broad-band probe-fed patch antenna with a W-shaped ground plane," *IEEE Trans. Antennas Propag.*, vol. 50, no. 6, pp. 827–831, Jun. 2002.

[12] G. Westfall and K.-B. Stephenson, "Antenna with stepped ground plane," U.S. Patent 6 014 114, Jan. 2000.

[13] T. Sarkar, A. Ghosh, L. L. K. Singh, S. Chattopadhyay, and C.-Y.-D. Sim, "DGS-integrated air-loaded wideband microstrip antenna for X- and Ku-band," *IEEE Antennas Wireless Propag. Lett.*, vol. 19, no. 1, pp. 114–118, Jan. 2020.

[14] C. Kumar and D. Guha, "Asymmetric geometry of defected ground structure for rectangular microstrip: A new approach to reduce its cross-polarized fields," *IEEE Trans. Antennas Propag.*, vol. 64, no. 6, pp. 2503–2506, Jun. 2016.

[15] M. I. Pasha, C. Kumar, and D. Guha, "Simultaneous compensation of microstrip feed and patch by defected ground structure for reduced cross-polarized radiation," *IEEE Trans. Antennas Propag.*, vol. 66, no. 12, pp. 7348–7352, Dec. 2018.

[16] M. I. Pasha, C. Kumar, and D. Guha, "Mitigating high cross-polarized radiation issues over the diagonal planes of microstrip patches," *IEEE Trans. Antennas Propag.*, vol. 68, no. 6, pp. 4950–4954, Jun. 2020.

[17] S. Rafidul, D. Guha, and C. Kumar, "Sources of cross-polarized radiation in microstrip patches: Multiparametric identification and insights for advanced engineering," *IEEE Antennas Propag. Mag.*, vol. 65, no. 2, pp. 92–103, Apr. 2023.

[18] X. Zhang and L. Zhu, "Patch antennas with loading of a pair of shorting pins toward flexible impedance matching and low cross polarization," *IEEE Trans. Antennas Propag.*, vol. 64, no. 4, pp. 1226–1233, Apr. 2016.

[19] C. Kumar and D. Guha, "Higher mode discrimination in a rectangular patch: New insight leading to improved design with consistently low cross-polar radiations," *IEEE Trans. Antennas Propag.*, vol. 69, no. 2, pp. 708–714, Feb. 2021.

[20] D. Ghosh et al., "Physical and quantitative analysis of compact rectangular microstrip antenna with shorted non-radiating edges for reduced cross-polarized radiation using modifi ed cavity model," *IEEE Antennas Propag. Mag.*, vol. 56, no. 4, pp. 61–72, Aug. 2014.

[21] Z. Wang, J. Liu, and Y. Long, "A simple wide-bandwidth and high-gain microstrip patch antenna with both sides shorted," *IEEE Antennas Wireless Propag. Lett.*, vol. 18, no. 6, pp. 1144–1148, Jun. 2019.

[22] C. Kumar, C. Sarkar, and D. Guha, "Radiating mode induced cross-polar source in microstrip patch: Identification and solution," *IEEE Antennas Wireless Propag. Lett.*, vol. 21, no. 10, pp. 2080–2084, Oct. 2022.

[23] S. Liu, D. Yang, Y. Chen, X. Zhang, and Y. Xiang, "High isolation and low cross-polarization of low-profile dual-polarized antennas via metasurface mode optimization," *IEEE Trans. Antennas Propag.*, vol. 69, no. 5, pp. 2999–3004, May 2021.

[24] C. Kumar, V. S. Kumar, and D. Venkataramana, "A large microstrip patch array with a simplified feed network: a low cross-polarized design," *IEEE Antennas Propag. Mag.*, vol. 61, no. 5, pp. 105–111, Oct. 2019.

[25] S. Gao, L. W. Li, M. S. Leong, and T. S. Yeo, "A broad-band dual-polarized microstrip patch antenna with aperture coupling," *IEEE Trans. Antennas Propag.*, vol. 51, no. 4, pp. 898–900, Apr. 2004.

[26] Q. Rao and R. H. Johnston, "Modified aperture coupled microstrip antenna," *IEEE Trans. Antennas Propag.*, vol. 52, no. 12, pp. 3397–3401, Dec. 2004.

[27] C. Y. D. Sim, C. C. Chang, and J. S. Row, "Dual-feed dual-polarized patch antenna with low cross polarization and high isolation," *IEEE Trans. Antennas Propag.*, vol. 57, no. 10, pp. 3321–3324, Oct. 2009.

[28] D. Guha, C. Kumar, and S. Biswas, *Defected Ground Structure (DGS) Based Antennas*, 1st ed. Hoboken, NJ, USA: Wiley, 2022.

[29] S. Bhardwaj and Y. Rahmat-Samii, "Revisiting the generation of cross-polarization in rectangular patch antennas: A near-field approach," *IEEE Antennas Propag. Mag.*, vol. 56, no. 1, pp. 14–38, Feb. 2014.

[30] D. Dutta, D. Guha, and C. Kumar, "A concept of advanced design governed by theoretically predicted current distributions on the ground plane beneath an aperture-fed microstrip antenna," *IEEE Open J. Antennas Propag.*, vol. 4, pp. 461–471, 2023.

[31] *High Frequency Structure Simulator (HFSS) V.2022R1*, ANSYS, Canonsburg, PA, USA, 2022.

[32] A. C. Ludwig, "The definition of cross polarization," *IEEE Trans. Antennas Propag.*, vol. AP-21, no. 1, pp. 116–119, Jan. 1973.
[33] D. Guha, A. Banerjee, C. Kumar, and Y. M. M. Antar, "Higher order mode excitation for high-gain broadside radiation from cylindrical dielectric resonator antennas," *IEEE Trans. Antennas Propag.*, vol. 60, no. 1, pp. 71–77, Jan. 2012.
[34] H. A. Wheeler, "The radian sphere around a small antenna," *Proc. IRE*, vol. 47, no. 8, pp. 1325–1331, Aug. 1959.

SK RAFIDUL (Graduate Student Member, IEEE) was born in India. He received the B.Tech. and M.Tech. degrees in radio physics and electronics from the University of Calcutta, India, in 2015 and 2017, respectively, where he is currently pursuing the Ph.D. degree with the Institute of Radio Physics and Electronics. He is also working on high gain resonance cavity antenna and techniques for antenna gain enhancement. His current research interests include microstrip and dielectric resonator antennas with suppressed cross-polarized radiation over 3-D radiation planes for space-borne and mobile applications. He was a recipient of the Antenna and Propagation Society Ph.D. Travel Grant Award in IEEE AP-S/URSI 2022 Conference, Denver, USA. He was the Secretary of IEEE APS Student Branch Chapter, Calcutta University from 2020 to 2022. He is currently serving as the Chair of IEEE APS Student Branch Chapter, Calcutta University. He is an Active Volunteer of the IEEE.

CHANDRAKANTA KUMAR (Senior Member, IEEE) received the M.Tech. and Ph.D. degrees in radio physics and electronics from the University of Calcutta, India, and completed Space Studies Program from International Space University, Strasbourg, France.

He joined Communication Systems Group, U R Rao Satellite Centre, ISRO, Bengaluru, in 2001. He has designed antenna systems of about twenty spacecrafts, including Mars Orbiter Mission, Chandrayaan-1 and 2, Moon Impact Probe. He also worked for the ground stations like 32-m diameter "Indian deep space network station" IDSN-32, satellite tracking antennas, and transportable tracking terminals. He served as the Deputy Project Director for RF Systems of Chandrayaan-2 Orbiter; and as the Project Manager for antenna systems of Chandrayaan-1, Moon Impact Probe, and ASTROSAT and GSAT-12 missions. He is a Fellow of the Indian National Academy of Engineering, the West Bengal Academy of Science and Technology, and the Institution of Electronics and Telecommunication Engineers. He has 145 technical publications, including 55 in IEEE journals/magazines to his credit and published a book on "*Defected Ground Structure Based Antennas*" (IEEE Press Willy, USA). He has supervised two Master and three Ph.D. theses. His present research areas are low cross-pol antennas, microwave photonic techniques, lightweight phased array antennas, and RF systems for spacecrafts.

Dr. Kumar is a recipient of "Young Scientist Merit Award-2009" and "Team Excellence Award-2008" from ISRO, and "Prof. S. N. Mitra Memorial Award-2011" and Hari Ramji Toshniwal Award-2018 from IETE, India. He also received 2nd Best Paper Award in InCAP 2019, Ahmedabad; the second and third Best Paper Awards in iAIM-2017, 'K U Limaye' Memorial Best Paper Awards in ISM-2008 and IRSI 2009 held in Bengaluru. He is currently serving as an Associate Editor of IEEE ANTENNAS AND WIRELESS PROPAGATION LETTERS and is on the board of reviewers of IEEE TRANSACTIONS ON ANTENNAS AND PROPAGATION, *IEEE Antennas and Propagation Magazine*, *IET Microwaves, Antennas & Propagation*. He is currently the Vice Chair of the IEEE Bangalore Section and the Chair-Elect of its AP-MTT joint chapter. He was the TPC and the Publication Chair of inaugural edition of B-HTC 2020 and served as the Organizing Chair of CONECCT-2021, 2022, and 2023 Conferences of IEEE Bangalore Section. He is an Active Volunteer of IEEE.

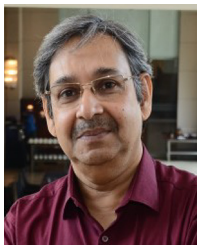

DEBATOSH GUHA (Fellow, IEEE) received the B.Tech. and M.Tech. degrees from the University of Calcutta in 1987 and 1989, respectively, and the Ph.D. degree in microwave engineering from University of Calcutta.

He started his career in Telecommunication Industry in India. He is a Professor of Radio Physics and Electronics with the University of Calcutta and also an Adjunct Professor with the National Institute of Technology Jaipur, India. He joined the University of Calcutta as an Assistant Professor in 1994. Later on, he spent about a couple of years with the Royal Military College of Canada, Kingston, ON, Canada as a Visiting Research Professor. He is also a Fellow of all four Indian National Academies for Science and Engineering which include the Indian National Science Academy; the Indian Academy of Sciences, Bengaluru; The National Academy of Sciences, Allahabad, India; and the Indian National Academy of Engineering. He has researched in developing microstrip and dielectric resonator antenna technologies. Defected ground structure-inspired antenna is one of his major areas of contribution. More than 200 technical papers in IEEE journals and conferences along with a couple of books on planar antenna published by IEEE Press/Wiley are to his credit. Several of his invented techniques are now commonly used by industries and the leading R&D Labs. A novel high gain wireless antenna developed by him has been a commercial product since 2007 in the North American market. He has mentored more than 23 doctoral and postdoctoral students over the last two decades. His current research interests include defected ground structure and metasurface induced antenna, hybrid subarray structures, solving cross-polarization issues for SAR, and advanced resonance cavity antenna techniques.

Prof. Guha is a recipient of some notable awards which include the IETE Ram Lal Wadhwa Award in 2016, the Raj Mittra Travel Grant Award in 2012, the URSI Young Scientist Award in 1996, and Jawaharlal Nehru Memorial Fund Prize in 1984. He served as an Associate Editor for IEEE TRANSACTIONS ON ANTENNAS AND PROPAGATION and IEEE ANTENNAS AND WIRELESS PROPAGATION LETTERS and he has been currently serving the IEEE AP-S AdCom as the Chair of AP-S Member and Geographic Activities Committee and the Co-Chair of the AP-S Technical Committee on Antenna Measurements. He served as a member of IEEE AP-S Fields Award Committee from 2017 to 2019. He has been serving as the Indian Chair URSI Commission B and the Representative of the Indian National Committee for URSI since 2014. He served the IEEE Kolkata Section as a Chair from 2013 to 2014, and the Founding Chair of AP/MTT-S Kolkata Chapter in 2004. He is a Co-Founder of a leading conference MAPCon (IEEE Microwaves Antennas and Propagation Conference) in India initiated in 2022. Prior to MAPCon, he conceptualized and established IEEE Applied Electromagnetics Conference in 2007 as a major biennial IEEE meeting in India and IEEE Indian Antenna Week as a yearly international workshop in 2010. He is an Abdul Kalam Technology Innovation National Fellow.